Investigating the Physical Properties of Thallium-Based Ternary TlXF₃ (X = Be, Sr) Fluoroperovskite Compounds for Prospective Applications

Gohar Ayub,[∇∇] Abdur Rauf,[∇∇] Mudasser Husain,* Ali Algahtani, Vineet Tirth, Tawfiq Al-Mughanam, Abdulaziz H. Alghtani, Nourreddine Sfina, Nasir Rahman,* Mohammad Sohail, Rajwali Khan, Ahmed Azzouz-Rached, Aurangzeb Khan, Nora Hamad Al-Shaalan, Sarah Alharthi, Saif A. Alharthy, and Mohammed A. Amin

Read Online

ACCESS | Metrics & More | Article Recommendations

ABSTRACT: In the present work, several properties of fluoroperovskites are computed and examined through the approximations of trans- and blaha-modified Becke−Johnson (TB-mBJ) and generalized gradient approximation of Perdew−Burke−Ernzerhof (GGA-PBE) integrated within density functional theory (DFT). The lattice parameters for cubic TlXF₃ (X = Be, Sr) ternary fluoroperovskite compounds at an optimized state are examined and their values are used to calculate the fundamental physical properties. TlXF₃ (X = Be and Sr) cubic fluoroperovskite compounds contain no inversion symmetry and are thus a non-centrosymmetric system. The phonon dispersion spectra confirm the thermodynamic stability of these compounds. The results of electronic properties clarify that both the compounds possess a 4.3 eV of indirect band gap from M−X for TlBeF₃ and a direct band gap of 6.03 eV from X−X for TlSrF₃, which display that both compounds are insulators. Furthermore, the dielectric function is considered to explore optical properties like reflectivity, refractive index, absorption coefficient, etc., and the different types of transitions between the bands were investigated by using the imaginary part of the dielectric function. Mechanically, the compounds of interest are computed to be stable and possess high bulk modulus values, and the ratio of "G/B" is higher than "1", which indicates the strong and ductile nature of the compound. Based on our computations for the selected materials, we deem an efficient application of these compounds in an industrial application, which will provide a reference for future work.
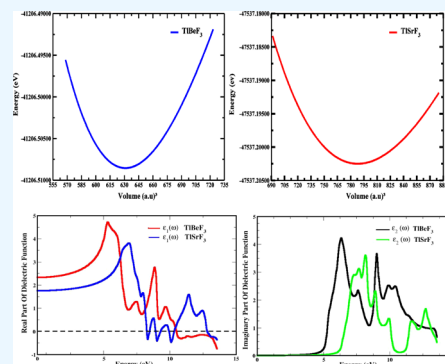
1. INTRODUCTION

The materials having ABX₃ stoichiometry show a family of perovskite-type structures where "A" and "B" are metallic cations, while "X" is an anion. ABF₃ shows the fluoroperovskite compounds, which is a subgroup of the perovskite family in which "X" is replaced by "F" in ABX₃. It possesses a very simple crystalline structure and has great importance and uses in a wide range of fields. The fluoroperovskite compounds have found applications in radiation dosimeters,[1] optical properties,[2−7] tunable laser,[8] ferro-electricity,[9] high-temperature super-ionic behavior,[10] semi-conductivity,[11−14] anti-ferromagnetism,[15] catalytic activity,[16] piezoelectricity,[17,18] and super-conducting properties.[19,20] A stable structure of perovskite compounds can be formed by taking the transition elements on "A" or "B" sites.[21−24] The crystalline structure of an exciting group of fluoroperovskite materials is mechanically stable and possesses exceptional optoelectronic capabilities that range from semiconducting (1−4 eV) to insulating (beyond 4 eV) in nature.[25−27] Recently, material scientists have shown a great

interest in fluoroperovskite compounds because of their unique desirable properties.[28−30] Rehman et al. investigated several physical properties of BeMF₃, M = Ti and V, using GGA within FP-LAPW with a simulation code of WIEN2K.[31] Some unique physical properties of Tl-based fluoroperovskite compounds TlXF₃ (X = Ca, Cd, Hg, and Mg) were reported by Khan et al. while using the ab initio method for density functional theory (DFT) calculations.[32] Many significant features, including ferroelectric, piezoelectric, and nonlinear optical capabilities, need a non-centrosymmetric structure. The selected TlXF₃ (X = Be and Sr) cubic fluoroperovskite compounds contain no inversion symmetry and are thus a non-
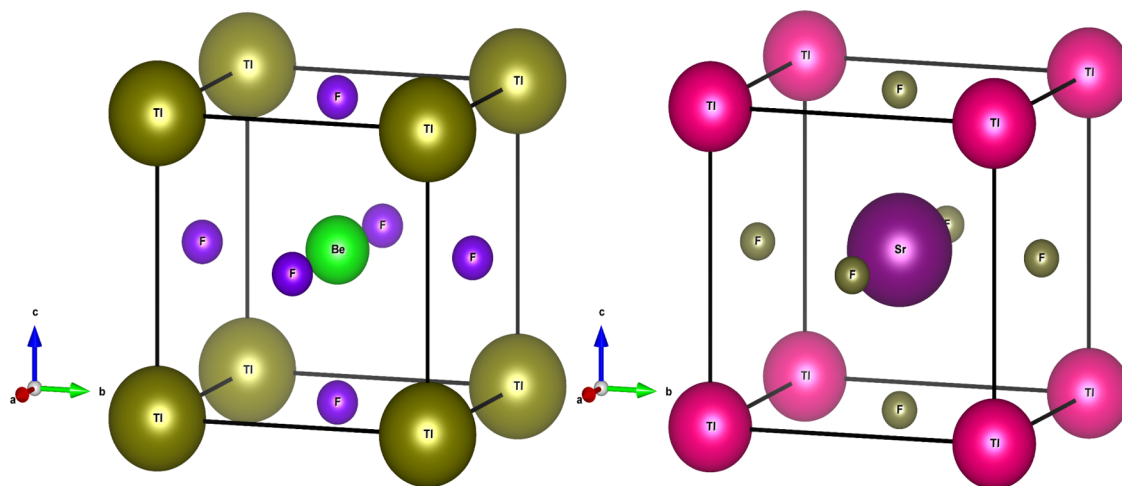
Figure 1. Description of the crystalline unit cell of ternary cubic $TlBeF_3$ and $TlSrF_3$ fluoroperovskite compounds.

centrosymmetric system. Optical lithography in semiconductors is subject to rising technological demands, and a shorter-wavelength lithographic light is needed for that. Thus, optical lithography steppers need lenses made of ultraviolet-transparent (UV-transparent) materials.[33−35] The best prospects for this use of perovskite-like fluorides with large band gaps is because, for lens materials, the cubic perovskite structure is preferred. After all, it lacks the birefringence that makes lens fabrication challenging.[36,37] To detect radiation, thallium-based compounds are being produced, and numerous studies have demonstrated their value in this use. These compounds' increased effective atomic number, caused by the presence of a thallium atom, increases the effectiveness of detection.[38] These compounds can be used in several electronic devices because of the complex composition of both elements "A" and "B" in $TlXF_3$ (X = Be, Sr) compounds. Up till now, no sufficient theoretical and experimental work exists on the structural, elastic, electronic, and optical properties of $TlXF_3$ (X = Be, Sr) compounds. To find out some of its physical properties, the $TlXF_3$ (X = Be and Sr) fluoroperovskite compounds are selected for the first time and various properties are calculated using WIEN2K, which will help scientists to investigate and confirm it experimentally.

2. COMPUTATIONAL METHODOLOGY

In this study, the WIEN2K simulation code is used in the computational approach with the DFT scheme,[39−41] and the scheme of FP-LAPW[42] is used to solve the equation of Kohn−Sham. In the case of many-body problems, this technique is the basic quantum mechanical procedure and is one of the most reliable approaches for studying physical properties.[43,44] The GGA and TB-mBJ[45] potential approximations can be dealt with by the use of the impact of physical properties. To explain matrix size, a parameter RMT $\times$ K_{max} = 8 is used in the calculation, where K_{max} gives information about the plane wave cutoff and RMT tells us about the smallest radii in the sphere. The chosen muffin tins (MTs) are approximately proportionate to the radii. The stable range of energy for the whole system lies between 10^{-3} Ry, where self-consistent calculations are known as "converged". The wave function within the valence spheres ranges up to l_{max} = 10 with the charge density having a value up to G_{max} = 14. For accurate and clear calculations, the Monkorst−Pack 3000 special k-points were

used in the Brillouin zone. Similarly, for an accurate value of bands and optical properties, the TB-mBJ approximation was used. The Birch−Murnaghan equation of states[46] was used for optimizing lattice parameters. Generally, the dielectric function $\varepsilon(\omega) = \varepsilon_1(\omega) + i\varepsilon_2(\omega)$ is used for investigating the optical properties. The established IRelast code by Morteza et al.[47] is used to calculate the cubic elastic constant (E_{cs}) and other mechanical properties of ternary $TlXF_3$ (X = Be and Sr) fluoroperovskite compounds.

3. INVESTIGATED RESULTS AND DISCUSSION

This section describes in detail the investigated results for structural, elastic, and optoelectronic properties for ternary cubic $TlXF_3$ (X = Be and Sr) fluoroperovskite compounds.

3.1. Structural Properties. The ternary $TlXF_3$ (X = Be and Sr) fluoroperovskites possess a cubic crystal structure as displayed in Figure 1, in which "Tl" atoms lie at (0, 0, 0), X = Be and Sr is at (0.5, 0.5, 0.5), and "F" takes the Wyckoff positions of either (0, 0.5, 0.5) or (0.5, 0, 0.5), or (0.5, 0.5, 0).

The fundamental structural properties are predicted from the fitted curves of the total energy of the primitive unit cell vs. the total volume of the primitive unit cell through the Birch−Mumaghan equation of state (EOS). The optimized points define the fundamental state of the crystals and are accompanied by the corresponding minimum volume, called the optimum volume, which is materialized to calculate the structural lattice parameters. Table 1 indicates the outcomes of structural optimized parameters. The fitted curves of structural optimization for $TlXF_3$ (X = Be and Sr) are displayed in Figure

Table 1. Values of Optimized Structural Parameters Computed for Ternary $TlXF_3$ (X = Be and Sr) Fluoroperovskite Compounds[a]

optimized structural values	$TlBeF_3$	$TlSrF_3$
a_0 (lattice constant)	4.5393	4.8879
B (bulk modulus)	49.2938	36.4548
B' (derivative of bulk modulus)	5.6198	5.0592
E_0 (ground state energy)	−41,206.508627	−47,537.202492
V_0 (ground state volume)	631.2132	788.0924

[a]The table displays the lattice constant "a_0" in Å, bulk modulus "B" in GPa, the (derivative of bulk modulus) B', the ground state energy E_0 in Ry, and the ground state volume "V_0" in (a.u)^3.
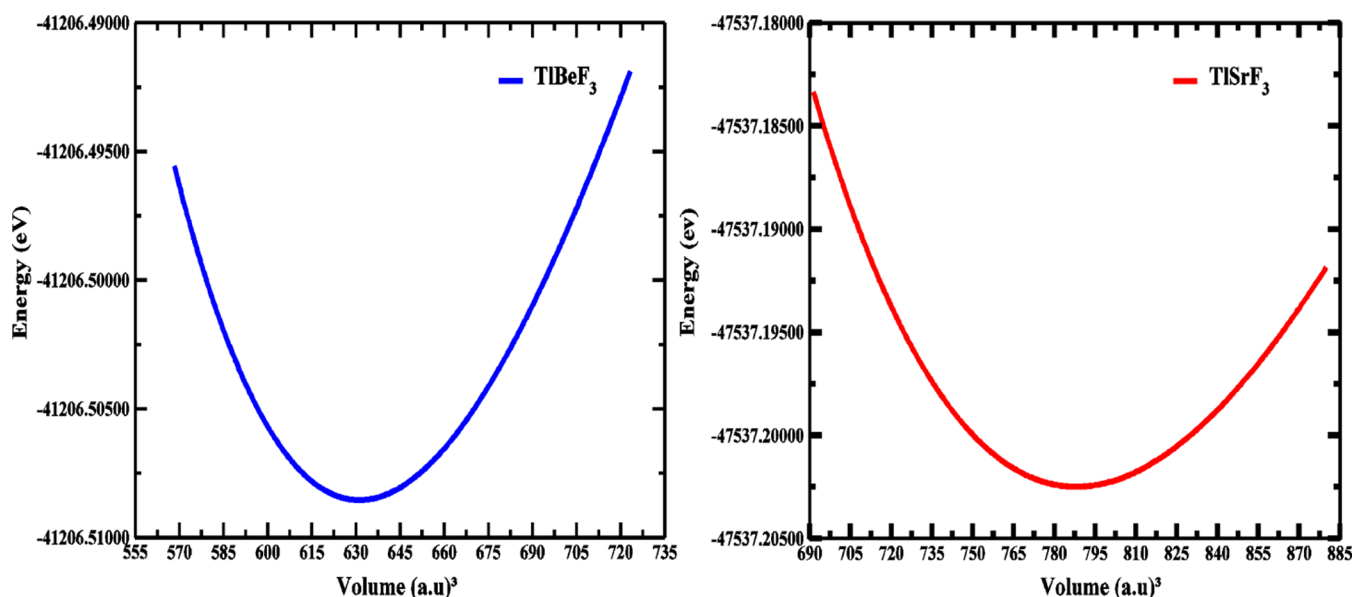
Figure 2. Optimized unit cell structure of ternary TlXF$_3$ (X = Be and Sr) fluoroperovskite compounds.

2 through the Birch−Mumaghan EOS. The equilibrium structural lattice parameters and the bulk modulus (B) of these materials amplify the potency, whereas the pressure derivative of "B" of a material is handy in finding the thermoplastic aspects. Hence, both parameters are worthy of being rated. Table 1 illustrates the investigated values of "B", which reduce as we move from TlBeF$_3$ to TlSrF$_3$. The bulk modulus value of TlBeF$_3$ is higher than that of TlSrF$_3$, which indicates that TlBeF$_3$ is harder than TlSrF$_3$.

3.2. Elastic Properties. In this study, the elastic constant "C_{ij}" and other elastic parameters for examining the mechanical properties of different materials are computed using the IRelast package. The decisive factor of elastic constant parameters gives information about the reaction to applied macroscopic stress. A physical link can be made by constants of elasticity "C_{ij}" between the active functioning of a material. It also explains the deformation shaped by the applied stress, and its restoration to the initial stage later than the applied stress has been observed.[48] The "C_{ij}" plays a vital role in materials, which gives important insights into structure stability, anisotropy, and bonding character of the atomic planes that are adjoining. In a cubic compound, three self-dependent elastic constants, C_{11}, C_{12}, and C_{44}, are tried to determine these parameters. The deformation created at any time in the cubic unit cell is applied by a suitable strain tensor, yielding an energy strain correlation. The IRelast package developed by Jamal Murtaza is utilized extremely efficiently. Table 2 gives the summary of "C_{ij}" and some other mechanical properties calculated from the elastic constant "C_{ij}" and bulk modulus "B". Calculations are optimistic. The criterion is $(C_{11} - C_{12}) > 0$; $(C_{11} + 2C_{12}) > 0$; $C_{44} > 0$; and "B" should be a prompt standard: $C_{12} < B < C_{11}$, this gives the mechanical stability necessary for cubical crystal systems.[49] Table 2 depicts the elastic parameters of the selected ternary TlXF$_3$ (X = Be, Sr) fluoroperovskite compound by using the IRelast calculation package. As is well known, no experimental results or theoretical findings for the elastic constant of the existing compound have been provided. Therefore, the calculated elastic properties can be used as a citation for further research work. The relation used

Table 2. Investigated Elastic Constants C_{ij} (C_{11}, C_{12}, C_{44} in GPa), Young's Modulus "E", Bulk Modulus "B", Shear Modulus "G", Reus's Shear Modulus (all in GPa), Poisson's Ratio "v", Pugh Ratio (B/G), and Anisotropy Factor "A" for Ternary TlXF$_3$ (X = Be and Sr) Fluoroperovskite Compounds

elastic parameters	TlBeF$_3$	TlSrF$_3$
C_{11} (GPa)	85.834366	92.182387
C_{12} (GPa)	91.265622	15.902439
C_{44} (GPa)	72.564401	6.944043
G_R	−7.193	10.321
E (Young's modulus)	98.808	49.480
G (shear modulus)	17.62977259	14.87155629
A_n (anisotropy factor)	−26.721	0.182
v (Poisson's ratio)	0.164	0.274
B/G (Pugh ratio)	2.777942809	2.451310359
B (GPa)	48.9745	36.4548

for the calculation of added elastic parameters A, G, and E are as follows

$$A = \frac{2C_{44}}{C_{11} - C_{12}} \tag{i}$$

$$G_v = \frac{1}{5}(C_{11} - C_{12} + 3C_{44}) \tag{ii}$$

$$G = \frac{1}{2}(G_v + G_R) \tag{iii}$$

$$v = \frac{3B - 2G}{2(2B + G)} \tag{iv}$$

$$E = \frac{9GB}{3B + G} \tag{v}$$

$$G_R = \frac{5C_{44}(C_{11} - C_{12})}{4C_{44} + 3(C_{11} - C_{12})} \tag{vi}$$

Here, the anisotropy factor is shown by "A" in eqs i and v. It is Poisson's ratio. Young's modulus in eq vi is represented by "E".
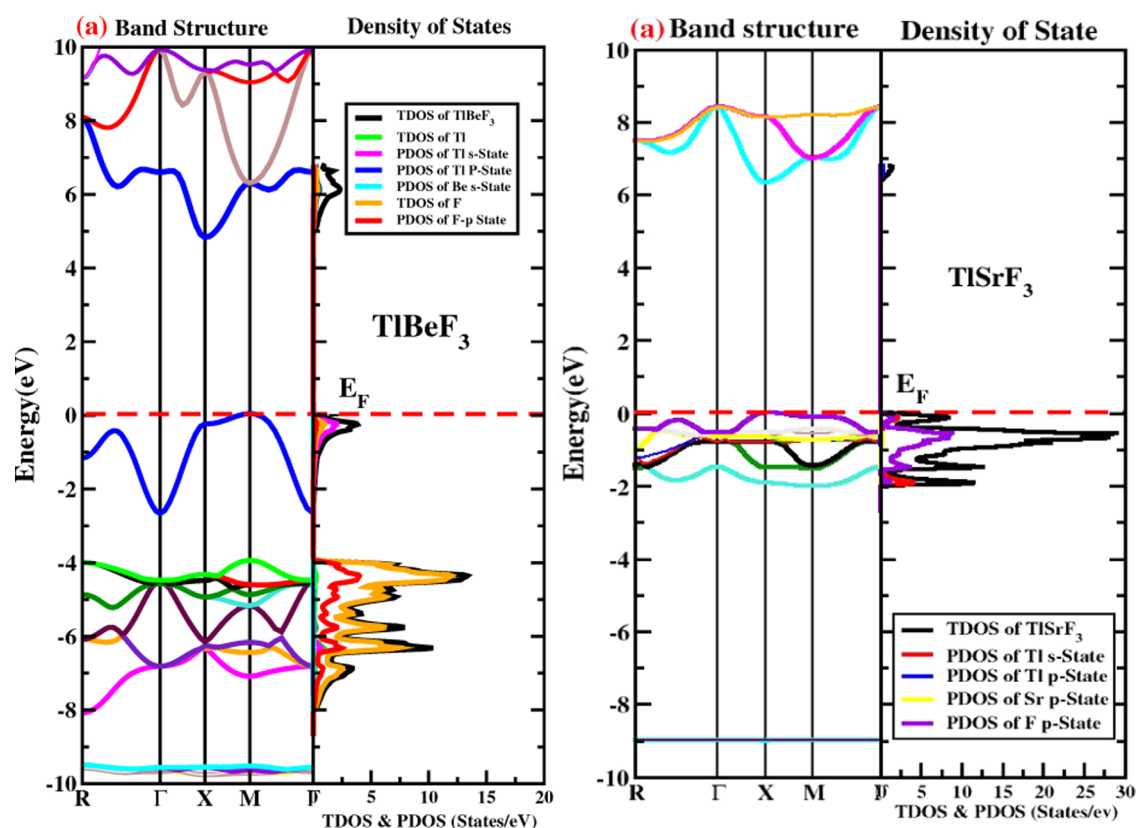
Figure 3. Fitted band structures and DOS from −10 eV up to 10 eV for ternary TlXF$_3$ (X = Be and Sr) fluoroperovskite compounds.

In eq iv, "G" gives Voigt's shear modulus following the "G" upper limit values. In eq vii, "G_R" shows Reus's shear modulus ensuring the lower bound of G. Table 2 verifies the positive value of bulk modulus and elastic constant for both compounds, which depicts that the compounds are mechanically stable. In the case of an isotropic compound, the value of "A" will be "1," the value other than "1" shows anisotropy, and the degree of the variations from "1" gives elastic anisotropy. In this work, the values of the anisotropy factor are −26.721 for TlBeF$_3$ and 0.182 for TlSrF$_3$. As both values are lesser than "1" therefore it shows anisotropic nature. The "E" value of a material is directly proportional to the stiffness of that material. The material will be stiffer if the value of "E" is higher. The information about bonding forces is given by Poisson's ratio (v). In the case of covalent materials, the value of "v" will be small (v < 0.1), and its value is 0.25 if the compound is ionic. In this study, the value of "v" is 0.48100 for TlBeF$_3$ and 0.57157 for TlSrF$_3$. Therefore, for the ternary TlXF$_3$ (X = Be, Sr) fluoroperovskite materials, the excessive role in intrabonding is ionic. The mechanical properties (ductility and brittleness) of TlBeF$_3$ and TlSrF$_3$ are explained by the computed "B/G" (Pugh ratio) and the standard Pugh's criteria are 1.75. The material will be ductile if the B/G ratio is greater than 1.75. As given in Table 2, the values for the "B/G" ratio are greater for both compounds, i.e., 2.77 for TlBeF$_3$ and 2.45 for TlSrF$_3$, thus both compounds are ductile. This is the earliest theoretical study of the elastic properties of these compounds and can be utilized as the reference data for further research work.

3.3. Band Structure and Density of States (DOS). The electronic band structure with principal symmetry points at zero pressure in the Brillouin zone is displayed in Figure 3. The energy band gap is given by the zero-energy difference next to the zone center C. Here, the given band gap along the X—X of the TlSrF$_3$ compound is direct and that along the M—X of the TlBeF$_3$ is indirect.

Figure 3 gives information about the total and partial densities of states, i.e., (T-DOS) and (P-DOS). The F-p state beneath the Fermi level gives a major contribution in the valance band, while small contributions by the Tl-s state and X states are observed.

3.4. Optical Properties. An important computational scheme for assessing a compound's optical properties is the FP-LAPW. We analyze the optical parameters of the mentioned substance TlXF$_3$ (X = Be, Sr) using the basic dielectric function equation. The optical behavior of different compounds in different photon energy ranges (0−15 eV) is fully explained. The mathematical expression of the various parameters of optical properties can be noted as

$$\varepsilon(\omega) = \varepsilon_1(\omega) + i\varepsilon_2(\omega) \tag{vii}$$

$$n(\omega) = \left[\frac{\varepsilon_1(w)}{2} + \frac{\sqrt{\varepsilon_1^{\,2}(\omega) + \varepsilon_2^{\,2}(\omega)}}{2} \right]^{1/2} \tag{viii}$$

$$k(\omega) = \left[\frac{-\varepsilon_1(w)}{2} + \frac{\sqrt{\varepsilon_1^{\,2}(\omega) + \varepsilon_2^{\,2}(\omega)}}{2} \right]^{1/2} \tag{ix}$$
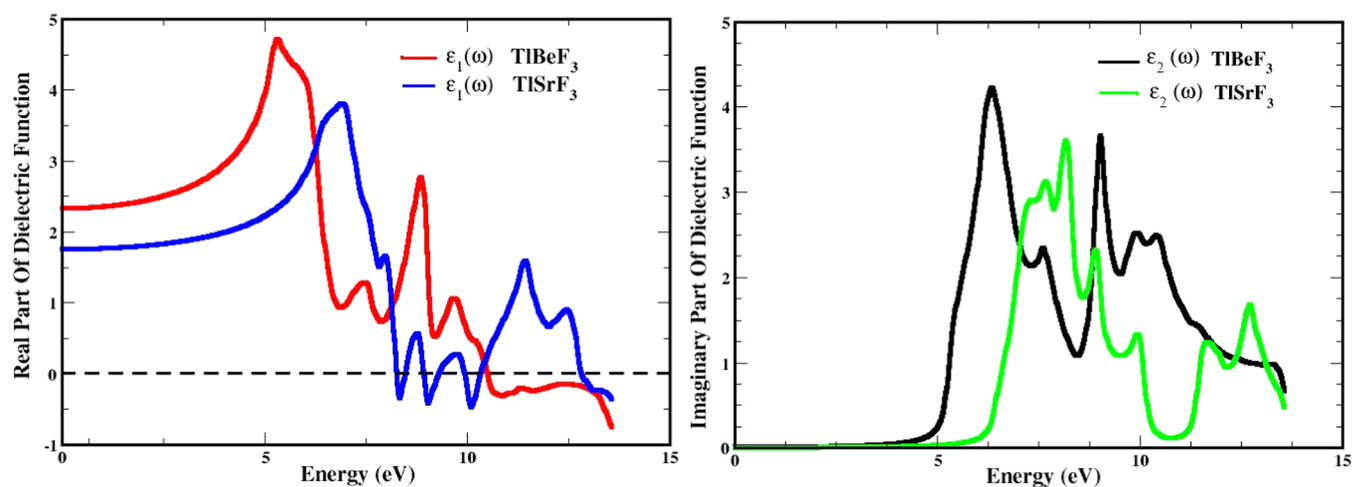
$$I(\omega) = \frac{2\omega}{c} k(\omega) \tag{x}$$

Figure 4. Computed real and imaginary parts of the dielectric function for ternary TlXF$_3$ (X = Be and Sr) fluoroperovskite compounds.
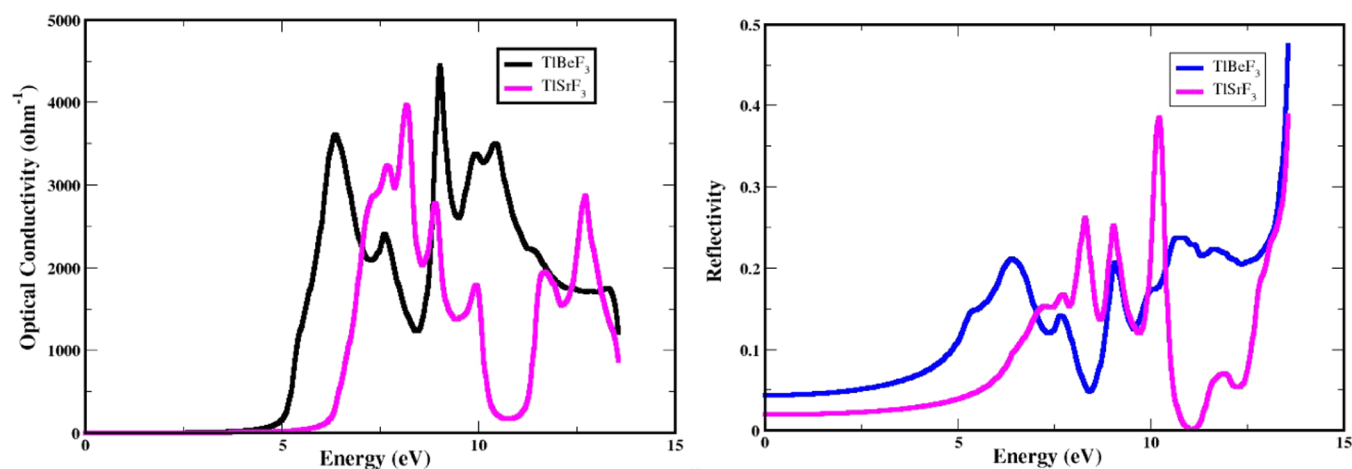

Figure 5. Investigated optical conductivity and reflectivity for ternary TlXF$_3$ (X = Be and Sr) fluoroperovskite compounds.

$$R(\omega) = \frac{(1-n)^2 + k^2}{(1+n)^2 + k^2} \tag{xi}$$

$$\sigma(\omega) = \frac{2Wev\hbar(\omega)}{E_o} \tag{xii}$$

where the equations from vii–xii show the $\varepsilon(\omega)$ (dielectric function), $n(\omega)$ (refractive index), $k(\omega)$ (extinction coefficient), $I(\omega)$ (absorption coefficient), $R(\omega)$ (reflectivity), and $\sigma(\omega)$ (optical conductivity).

3.4.1. Dielectric Function.

The real and imaginary components of the dielectric function are represented by ε_1 and ε_2 in eq i for the dielectric function and computed for both the TlXF$_3$ (X = Be, Sr) compounds. The spectra are shown in Figure 4. The electronic BS (band structure) of a material is strongly connected to the real component of the dielectric function, which is used to describe the degree to which a material can be polarized. The real part of the dielectric function also describes its dispersive behavior. On the one hand, the imaginary part demonstrates how the medium absorbs light. Figure 4 displays the optical activity of the compounds in the energy range from 0 to 15 eV, with several significant peaks.

3.4.2. Optical Conductivity and Optical Reflectivity.

The optical conductivity of a material describes the linkage between the induced current density and the magnitude of the induced electric field in a material for arbitrary frequencies. The complex dielectric function used to evaluate optical conductivity defines the conduction of electrons driven by an applied electromagnetic field and is the extension of electrical transport to optically high-frequency incident photons. The resultant spectrum is displayed in Figure 5. The TlBeF$_3$ and TlSrF$_3$ fluoroperovskite compounds are highly optical conductive at an incident energy of 8 and 7.5 eV, respectively. The TlXF$_3$ (X = Be, and Sr) compound is a fluoride perovskite with a cubic structure that has a large band gap and is suitable as a vacuum-ultraviolet-transparent (VUV-transparent) material for lenses in optical lithographic technology. Optical reflectivity is a direct measure of electrical response. The figure shows the reflectance of the selected compounds. It is clear from the figure that the zero-frequency reflectivity is 2.5 and 5% at 0 eV for TlBeF$_3$ and TlSrF$_3$ compounds, respectively. This is relatively unchanged up to 3.2 eV. The material ought to be transparent in this energy range, according to the small value of reflectivity and the absorption coefficient in the infrared and visible-light ranges. Also, due to its low reflectivity in contrast to some of the other metal fluorides, it might be more practical. The highest values of reflectivity are 49 and 40% for TlBeF$_3$ and TlSrF$_3$, respectively, at the same energy range of 13 eV.
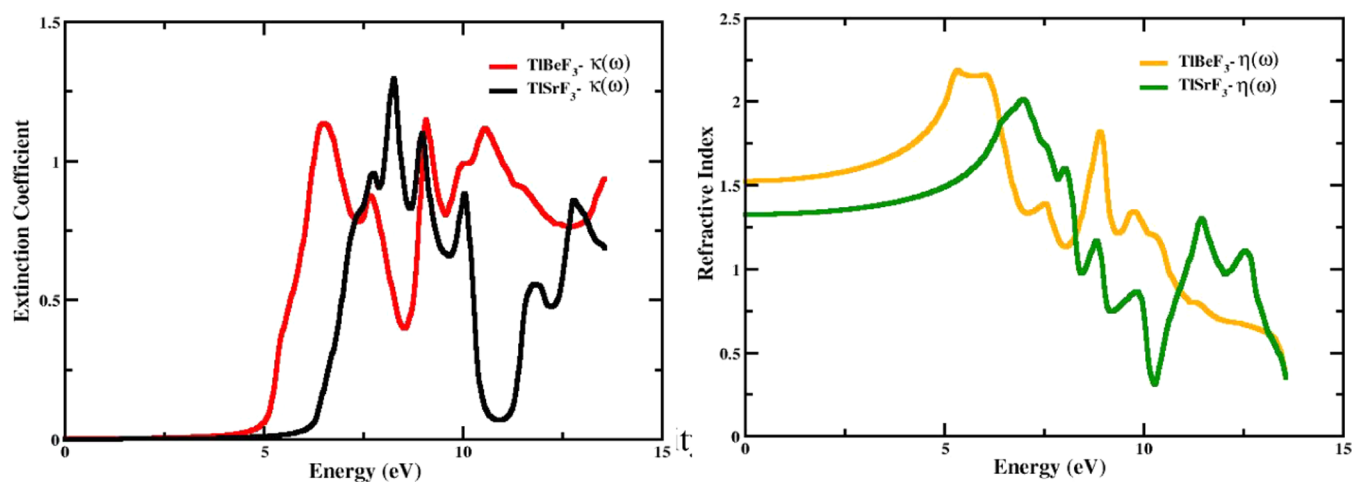
Figure 6. Extinction coefficient and refractive index computed for TlXF$_3$ (X = Be and Sr) fluoroperovskite compound.
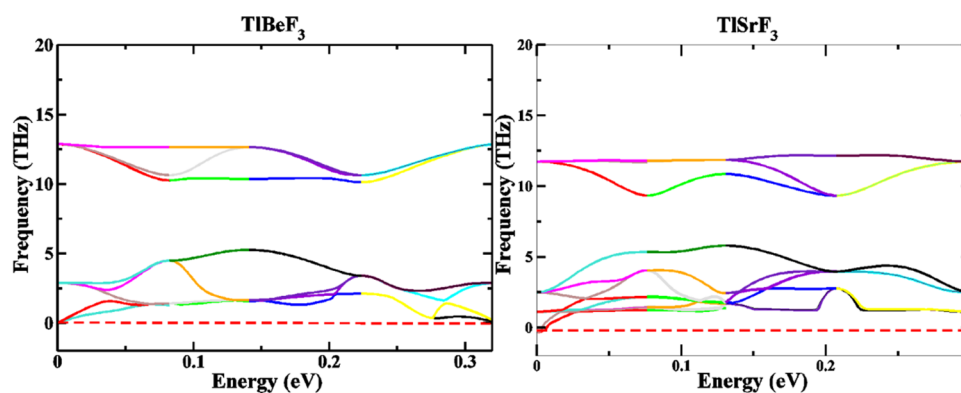

Figure 7. Predicted phonon spectra of ternary TlXF$_3$ (X = Be and Sr) cubic fluoroperovskite compounds.

3.4.3. Refractive Index and Extinction Coefficient. The $n(\omega)$ (refractive index) is a critical aspect to know when measuring the level of refraction, since it is extremely effective in photoelectric applications. A material's refractive index serves as a gauge for how light moves through it. High refractive indices cause light to move more slowly, which causes a proportionately greater change in the direction of the light inside the material. We have noticed that these compounds are anisotropic. Figure 6 presents the determined refractive index for the important compounds. At zero energy, it has been observed that TlBeF$_3$ and TlSrF$_3$ possess static reflection coefficients of 1.39 and 1.59, respectively. The maximum refractive index for TlBeF$_3$ is 2.2 at 6 eV, while that for TlSrF$_3$ is 2 at 7.5 eV. For the reported substance, the refractive index exceeds 1. A material's refractive index determines how much light is refracted as it passes through it. The higher the index, the more light is refracted. In general, the refractive index increases with every technique that increases the electron density in a substance. A property that governs how effectively a material absorbs or reflects radiations or light at a specific wavelength is termed the extinction coefficient. The figure displays the results of determining the extinction coefficient $k(x)$ for TlXF$_3$ (X = Be and Sr) compounds. The local maximum extinction coefficient of TlBeF$_3$ is about 1.2 at 6.0 eV and that of TlSrF$_3$ is about 1.32 at 8.0 eV.

3.5. Phononic Properties. Phonons have crucial roles in the dynamics of structural stability, thermal characteristics, and structural stability, all of which are crucial elements in the fundamental problems of materials science. The fundamental vibrational motion that occurs when a lattice of atoms or molecules vibrates consistently at a single frequency is known as a phonon in quantum mechanics. The investigated phonon dispersion spectra for ternary TlXF$_3$ (X = Be and Sr) cubic fluoroperovskite compounds are depicted in Figure 7.

It is very obvious from Figure 7 that all of the phonon dispersions curves existed at a positive value of frequency, and there exist no negative phonon spectra below 0 THz frequency. The existence of these curves at positive values of frequency confirms that both ternary TlXF$_3$ (X = Be and Sr) cubic fluoroperovskite compounds are thermodynamically stable.

4. CONCLUSIONS

The computational investigations of structural, electronic, elastic, and optoelectronic properties of TlXF$_3$ (X = Be, Sr) fluoroperovskites are carried out using the framework of DFT, and the approximations of GGA and TB-mBJ are employed for improving various properties. The optimized lattice constants are determined to be 4.5393 and 4.8879 Å for TlBeF$_3$ and TlSrF$_3$, respectively, which shows a stable cubic crystalline structure. The selected TlXF$_3$ (X = Be and Sr) cubic fluoroperovskite compounds contain no inversion symmetry and are thus a non-centrosymmetric system. The phonon spectra display the thermodynamic stability of the fluoroperovskite compounds. An indirect band gap from M−X for TlBeF$_3$ and a direct band gap from X−X exist for TlSrF$_3$,

displaying that both compounds are insulators. The investigated mechanical properties depict that the selected compounds are tough to scratch and mechanically stable. Based on the reported research for fluoroperovskite TlXF$_3$ (X = Be and Sr) cubic compounds, the applications at large scale can be deemed for these materials in advanced electronic devices and for energy storage purposes.

■ AUTHOR INFORMATION

Corresponding Authors

Mudasser Husain − *Department of Physics, University of Lakki Marwat, 28420 Lakki Marwat, Khyber Pakhtunkhwa, Pakistan*; Email: mudasserhusain01@gmail.com

Nasir Rahman − *Department of Physics, University of Lakki Marwat, 28420 Lakki Marwat, Khyber Pakhtunkhwa, Pakistan*; ⓞ orcid.org/0000-0003-1978-7280; Email: nasir@ulm.edu.pk

Authors

Gohar Ayub − *Department of Physics, University of Lakki Marwat, 28420 Lakki Marwat, Khyber Pakhtunkhwa, Pakistan*

Abdur Rauf − *Institute for Advanced Study (IAS), Shenzhen University, Shenzhen 518060 Guangdong, P. R. China; College of Physics and Optoelectronics Engineering, Shenzhen University, Shenzhen 518060 Guangdong, P. R. China*

Ali Algahtani − *Mechanical Engineering Department, College of Engineering, King Khalid University, Abha 61421, Saudi Arabia; Research Center for Advanced Materials Science (RCAMS), King Khalid University, Abha 61413 Asir, Saudi Arabia*

Vineet Tirth − *Mechanical Engineering Department, College of Engineering, King Khalid University, Abha 61421, Saudi Arabia; Research Center for Advanced Materials Science (RCAMS), King Khalid University, Abha 61413 Asir, Saudi Arabia;* ⓞ orcid.org/0000-0002-8208-7183

Tawfiq Al-Mughanam − *Department of Mechanical Engineering, College of Engineering, King Faisal University, Al-Ahsa 31982, Saudi Arabia*

Abdulaziz H. Alghtani − *Department of Mechanical Engineering, College of Engineering, Taif University, Taif 21944, Saudi Arabia*

Nourreddine Sfina − *College of Sciences and Arts in Mahayel Asir, Department of Physics, King Khalid University, Abha 61421, Saudi Arabia; Département de Physique, Faculté des Sciences de Monastir, Laboratoire de la Matière Condensée et des Nanosciences (LMCN), Université de Monastir, 5019 Monastir, Tunisia*

Mohammad Sohail − *Department of Physics, University of Lakki Marwat, 28420 Lakki Marwat, Khyber Pakhtunkhwa, Pakistan*

Rajwali Khan − *Department of Physics, University of Lakki Marwat, 28420 Lakki Marwat, Khyber Pakhtunkhwa, Pakistan*

Ahmed Azzouz-Rached − *Magnetic Materials Laboratory, Faculty of Exact Sciences, Djillali Liabes University of Sidi Bel-Abbes, Sidi Bel Abbès 22000, Algeria*

Aurangzeb Khan − *Department of Physics, Abdul Wali Khan University, 23200 Mardan, Pakistan*

Nora Hamad Al-Shaalan − *Department of Chemistry, College of Science, Princess Nourah Bint Abdulrahman University, Riyadh 11671, Saudi Arabia;* ⓞ orcid.org/0000-0002-5285-2155

Sarah Alharthi − *Department of Chemistry, College of Science and Center of Advanced Research in Science and Technology, Taif University, Taif 21944, Saudi Arabia*

Saif A. Alharthy − *Department of Medical Laboratory Sciences, Faculty of Applied Medical Sciences, King Abdulaziz University, Jeddah 21589, Saudi Arabia; King Fahd Medical Research Center, King Abdulaziz University, Jeddah 21589, Saudi Arabia*

Mohammed A. Amin − *Department of Chemistry, College of Science, Taif University, Taif 21944, Saudi Arabia*

Complete contact information is available at:
https://pubs.acs.org/10.1021/acsomega.3c00549

Author Contributions

▽▽G.A. and A.R. contributed equally to this work as first author and all authors have equal contribution in conceptualization investigations, analysis, writing original draft, review, and editing.

Notes

The authors declare no competing financial interest.

■ ACKNOWLEDGMENTS

■ REFERENCES

(1) Dotzler, C.; Williams, G. V. M.; Edgar, A. Radiation-Induced Optically and Thermally Stimulated Luminescence in RbCdF3 and RbMgF3. *Curr. Appl. Phys.* **2008**, *8*, 447−450.

(2) Hörsch, G.; Paus, H. J. A New Color Center Laser on the Basis of Lead-Doped KMgF3. *Opt. Commun.* **1986**, *60*, 69−73.

(3) Saddique, J.; Husain, M.; Rahman, N.; Khan, R.; Iqbal, A.; Sohail, M.; Khattak, S. A.; Khan, S. N.; Khan, A. A.; Reshak, A. H.; et al. Modeling Structural, Elastic, Electronic and Optical Properties of Ternary Cubic Barium Based Fluoroperovskites MBaF3 (M = Ga and In) Compounds Based on DFT. *Mater. Sci. Semicond. Process.* **2022**, *139*, No. 106345.

(4) Shah, S. A.; Husain, M.; Rahman, N.; Sohail, M.; Khan, R.; Khan, A. A.; Ullah, A.; Abdelmohsen, S. A. M.; Abdelbacki, A. M. M.; El-Sabrout, A. M.; et al. Insight into the Exemplary Structural, Elastic, Electronic and Optical Nature of GaBeCl 3 and InBeCl 3: A DFT Study. *RSC Adv.* **2022**, *12*, 8172−8177.

(5) Habib, A.; Husain, M.; Sajjad, M.; Rahman, N.; Khan, R.; Sohail, M.; Ali, I. H.; Iqbal, S.; Khan, M. I.; Ebraheem, S. A. M.; et al. Insight into the Exemplary Physical Properties of Zn-Based Fluoroperovskite Compounds XZnF3 (X = Al, Cs, Ga, In) Employing Accurate GGA Approach: A First-Principles Study. *Materials* **2022**, *15*, No. 2669.

(6) Rahman, N.; Husain, M.; Yang, J.; Sajjad, M.; Murtaza, G.; Haq, M. U.; Habib, A.; Rauf, A.; Karim, A.; Nisar, M.; et al. First Principle Study of Structural, Electronic, Optical and Mechanical Properties of Cubic Fluoro-Perovskites:(CdXF 3, X = Y, Bi). *Eur. Phys. J. Plus* **2021**, *136*, No. 347.

(7) Husain, M.; Rahman, N.; Khan, R.; Zulfiqar, S.; Khattak, S. A.; Khan, S. N.; Sohail, M.; Iqbal, A.; Reshak, A. H.; Khan, A. Structural, Electronic, Elastic, and Magnetic Properties of NaQF3 (Q = Ag, Pb,

Rh, and Ru) Flouroperovskites: A First-principle Outcomes. *Int. J. Energy Res.* **2022**, *46*, 2446−2453.

(8) Manaa, H.; Guyot, Y.; Moncorge, R. Spectroscopic and Tunable Laser Properties of Co 2+-Doped Single Crystals. *Phys. Rev. B* **1993**, *48*, 3633−3645.

(9) Berastegui, P.; Hull, S.; Eriksson, S. G. A Low-Temperature Structural Phase Transition in CsPbF3. *J. Phys.: Condens. Matter* **2001**, *13*, 5077−5088.

(10) Chadwick, A. V.; Strange, J. H.; Ranieri, G. A.; Terenzi, M. Studies of Ionic Motion in Perovskite Fluorides. *Solid State Ionics* **1983**, *9−10*, 555−558.

(11) Mubarak, A. A.; Mousa, A. A. The Electronic and Optical Properties of the Fluoroperovskite BaXF3 (X = Li, Na, K, and Rb) Compounds. *Comput. Mater. Sci.* **2012**, *59*, 6−13.

(12) Benmhidi, H.; Rached, H.; Rached, D.; Benkabou, M. Ab Initio Study of Electronic Structure, Elastic and Transport Properties of Fluoroperovskite LiBeF3. *J. Electron. Mater.* **2017**, *46*, 2205−2210.

(13) Sajjad, M.; Khan, U. A.; Ullah, H.; Alhodaib, A.; Amami, M.; Tirth, V.; Zaman, A.; et al. Structural, Electronic, Magnetic and Elastic Properties of Xenon-Based Fluoroperovskites XeMF 3 (M = Ti, V, Zr, Nb) via DFT Studies. *RSC Adv.* **2022**, *12*, 27508−27516.

(14) Mousa, A. A.; Mahmoud, N. T.; Khalifeh, J. M. The Electronic and Optical Properties of the Fluoroperovskite XLiF3 (X = Ca, Sr, and Ba) Compounds. *Comput. Mater. Sci.* **2013**, *79*, 201−205.

(15) Vaitheeswaran, G.; Kanchana, V.; Kumar, R. S.; Cornelius, A. L.; Nicol, M. F.; Svane, A.; Christensen, N. E.; Eriksson, O. High-Pressure Structural Study of Fluoro-Perovskite CsCdF 3 up to 60 GPa: A Combined Experimental and Theoretical Study. *Phys. Rev. B* **2010**, *81*, No. 075105.

(16) Koonce, C. S.; Cohen, M. L.; Schooley, J. F.; Hosler, W. R.; Pfeiffer, E. R. Superconducting Transition Temperatures of Semiconducting SrTi O 3. *Phys. Rev.* **1967**, *163*, 380−390.

(17) Wang, H.; Wang, B.; Li, Q.; Zhu, Z.; Wang, R.; Woo, C. H. First-Principles Study of the Cubic Perovskites Bi M O 3 (M = Al, Ga, In, and Sc). *Phys. Rev. B* **2007**, *75*, No. 245209.

(18) Baettig, P.; Schelle, C. F.; LeSar, R.; Waghmare, U. V.; Spaldin, N. A. Theoretical Prediction of New High-Performance Lead-Free Piezoelectrics. *Chem. Mater.* **2005**, *17*, 1376−1380.

(19) Bouhemadou, A.; Khenata, R. Ab Initio Study of the Structural, Elastic, Electronic and Optical Properties of the Antiperovskite SbNMg3. *Comput. Mater. Sci.* **2007**, *39*, 803−807.

(20) Dimov, N.; Nishimura, A.; Chihara, K.; Kitajou, A.; Gocheva, I. D.; Okada, S. Transition Metal NaMF3 Compounds as Model Systems for Studying the Feasibility of Ternary Li-MF and Na-MF Single Phases as Cathodes for Lithium−Ion and Sodium−Ion Batteries. *Electrochim. Acta* **2013**, *110*, 214−220.

(21) Mubarak, A. A.; Al-Omari, S. First-Principles Calculations of Two Cubic Fluoropervskite Compounds: RbFeF3 and RbNiF3. *J. Magn. Magn. Mater.* **2015**, *382*, 211−218.

(22) Erum, N.; Iqbal, M. A. Mechanical and Magneto-Opto-Electronic Investigation of Transition Metal Based Fluoro-Perovskites: An Ab-Initio DFT Study. *Solid State Commun.* **2017**, *264*, 39−48.

(23) Raja, A.; Annadurai, G.; Daniel, D. J.; Ramasamy, P. Synthesis, Optical and Thermal Properties of Novel Tb3+ Doped RbCaF3 Fluoroperovskite Phosphors. *J. Alloys Compd.* **2016**, *683*, 654−660.

(24) Khan, H.; Sohail, M.; Rahman, N.; Hussain, M.; Khan, A.; Hegazy, H. H.; et al. Theoretical Study of Different Aspects of Al-Based Fluoroperovskite AlMF3 (M = Cu, Mn) Compounds Using TB-MBJ Potential Approximation Method for Generation of Energy. *Results Phys.* **2022**, *42*, No. 105982.

(25) Xue, S.; Shang, J.; Pu, X.; Cheng, H.; Zhang, L.; Wang, C.; Lee, C.-S.; Tang, Y. Dual Anionic Doping Strategy towards Synergistic Optimization of Co9S8 for Fast and Durable Sodium Storage. *Energy Storage Mater.* **2023**, *55*, 33−41.

(26) Ji, B.; Gou, J.; Zheng, Y.; Pu, X.; Wang, Y.; Kidkhunthod, P.; Tang, Y. Coordination Chemistry of Large-size Yttrium Single-atom Catalysts for Oxygen Reduction Reaction. *Adv. Mater.* **2023**, No. 2300381.

(27) Fu, M.; Chen, W.; Lei, Y.; Yu, H.; Lin, Y.; Terrones, M. Biomimetic Construction of Ferrite Quantum Dot/Graphene Heterostructure for Enhancing Ion/Charge Transfer in Supercapacitors. *Adv. Mater.* **2023**, No. 2300940.

(28) Zhang, X.; Tang, Y.; Zhang, F.; Lee, C. A Novel Aluminum−Graphite Dual-ion Battery. *Adv. Energy Mater.* **2016**, *6*, No. 1502588.

(29) Wang, M.; Jiang, C.; Zhang, S.; Song, X.; Tang, Y.; Cheng, H.-M. Reversible Calcium Alloying Enables a Practical Room-Temperature Rechargeable Calcium-Ion Battery with a High Discharge Voltage. *Nat. Chem.* **2018**, *10*, 667−672.

(30) Tang, Y.; Wang, L.; Ji, B.; Zheng, Y. Asymmetric Coordination of Iridium Single-atom IrN3O Boosting Formic Acid Oxidation Catalysis. *Angew. Chem., Int. Ed.* **2023**, *62*, No. e202301711.

(31) Husain, M.; Ahmad, M. S.; Rahman, N.; Sajjad, M.; Rauf, A.; Habib, A.; Haq, M. U.; Nisar, M.; Hussain, A.; Imran, M. First Principle Study Of The Structural, Electronic, And Mechanical Properties Of Cubic Fluoroperovskites: (Znxf3, X = Y, Bi). *Fluoride* **2020**, *53*, 657−667.

(32) Khan, S.; Zaman, S. U.; Ahmad, R.; Mehmood, N.; Arif, M.; Kim, H. J. Ab Initio Investigations of Structural, Elastic, Electronic and Optical Properties of the Fluoroperovskite TlXF3 (X = Ca, Cd, Hg, and Mg) Compounds. *Mater. Res. Express* **2019**, *6*, No. 125923.

(33) Nishimatsu, T.; Terakubo, N.; Mizuseki, H.; Kawazoe, Y.; Pawlak, D. A.; Shimamura, K.; Fukuda, T. Band Structures of Perovskite-like Fluorides for Vacuum-Ultraviolet-Transparent Lens Materials. *Jpn. J. Appl. Phys.* **2002**, *41*, L365−L367.

(34) Fu, M.; Zhuang, Q.; Yu, H.; Chen, W. MnCo2S4 Nanosheet Arrays Modified with Vermicular Polypyrrole for Advanced Free-Standing Flexible Electrodes. *Electrochim. Acta* **2023**, *447*, No. 142167.

(35) Wang, S.; Wang, B.; He, S.; Wang, Y.; Cheng, J.; Li, Y. Enhancing the Photovoltaic Performance of Planar Heterojunction Perovskite Solar Cells via Introducing Binary-Mixed Organic Electron Transport Layers. *New J. Chem.* **2023**, *47*, 5048−5055.

(36) Wei, Y.; Chen, C.; Tan, C.; He, L.; Ren, Z.; Zhang, C.; Peng, S.; Han, J.; Zhou, H.; Wang, J. High-Performance Visible to Near-Infrared Broadband Bi2O2Se Nanoribbon Photodetectors. *Adv. Opt. Mater.* **2022**, *10*, No. 2201396.

(37) Li, G.; Huang, S.; Li, K.; Zhu, N.; Zhao, B.; Zhong, Q.; Zhang, Z.; Ge, D.; Wang, D. Near-Infrared Responsive Z-Scheme Heterojunction with Strong Stability and Ultra-High Quantum Efficiency Constructed by Lanthanide-Doped Glass. *Appl. Catal., B* **2022**, *311*, No. 121363.

(38) Hawrami, R.; Ariesanti, E.; Burger, A.; Sellin, P. Latest Growth of Large Diameter Tl-Based Elpasolite Scintillation Crystals. *Opt. Mater.* **2022**, *128*, No. 112324.

(39) Bouhmaidi, S.; Marjaoui, A.; Talbi, A.; Zanouni, M.; Nouneh, K.; Setti, L. A DFT Study of Electronic, Optical and Thermoelectric Properties of Ge-Halide Perovskites CsGeX3 (X = F, Cl and Br). *Comput. Condens. Matter* **2022**, *31*, No. e00663.

(40) Obot, I. B.; Macdonald, D. D.; Gasem, Z. M. Density Functional Theory (DFT) as a Powerful Tool for Designing New Organic Corrosion Inhibitors. Part 1: An Overview. *Corros. Sci.* **2015**, *99*, 1−30.

(41) Zhang, G.; Musgrave, C. B. Comparison of DFT Methods for Molecular Orbital Eigenvalue Calculations. *J. Phys. Chem. A* **2007**, *111*, 1554−1561.

(42) Petersen, M.; Wagner, F.; Hufnagel, L.; Scheffler, M.; Blaha, P.; Schwarz, K. Improving the Efficiency of FP-LAPW Calculations. *Comput. Phys. Commun.* **2000**, *126*, 294−309.

(43) Bagayoko, D. Understanding Density Functional Theory (DFT) and Completing It in Practice. *AIP Adv.* **2014**, *4*, No. 127104.

(44) Argaman, N.; Makov, G. Density Functional Theory: An Introduction. *Am. J. Phys.* **2000**, *68*, 69−79.

(45) Kadim, G.; Masrour, R.; Jabar, A. A Comparative Study between GGA, WC-GGA, TB-MBJ and GGA+ U Approximations on Magnetocaloric Effect, Electronic, Optic and Magnetic Properties of BaMnS2 Compound: DFT Calculations and Monte Carlo Simulations. *Phys. Scr.* **2021**, *96*, No. 45804.

(46) Tyuterev, V. G.; Vast, N. Murnaghan's Equation of State for the Electronic Ground State Energy. *Comput. Mater. Sci.* **2006**, *38*, 350−353.

(47) Reshak, A. H.; Jamal, M. DFT Calculation for Elastic Constants of Orthorhombic Structure within WIEN2K Code: A New Package (Ortho-Elastic). *J. Alloys Compd.* **2012**, *543*, 147−151.

(48) Huntington, H. B. The Elastic Constants of Crystals. In *Solid State Physics*; Elsevier, 1958; Vol. 7, pp 213−351.

(49) Pugh, S. F. XCII. Relations between the Elastic Moduli and the Plastic Properties of Polycrystalline Pure Metals. *London, Edinburgh Dublin Philos. Mag. J. Sci.* **1954**, *45*, 823−843.